Geochemical Perspectives Letters

Fast REE re-distribution in mantle clinopyroxene *via* reactive melt infiltration

G. Borghini[1*], P. Fumagalli[1], F. Arrigoni[1], E. Rampone[2], J. Berndt[3], S. Klemme[3], M. Tiepolo[1]

https://doi.org/10.7185/geochemlet.2323

Abstract

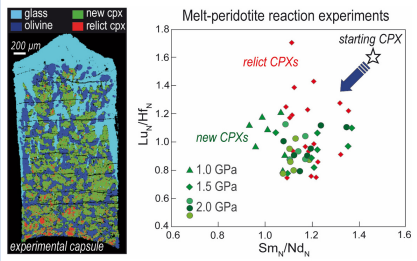

Melt-mineral interactions may strongly affect the mineralogy and chemistry of the upper mantle. Although the grain-scale processes governing the interaction have been theoretically investigated, the efficiency of melt-rock reaction in re-distributing trace elements in mantle clinopyroxene still remains to be experimentally evaluated. We performed high pressure reaction experiments at 1–2 GPa, 1200–1350 °C, on homogeneous mixtures of LREE-depleted clinopyroxene, San Carlos olivine and an Enriched-MORB glass. Melt-peridotite reaction leads to textural replacement of mantle clinopyroxene by dissolution and precipitation as a function of temperature and run duration. Experimental results indicate that rapid modification of the REE signature of mantle clinopyroxene occurs not only *via* dissolution and precipitation but even *via* trace element diffusion within unreacted crystal relicts. The extent of reacted melt crystallisation influences the REE fractionation in modified clinopyroxene. Aided by a high reaction rate, local chemical equilibrium between clinopyroxene and melt can be approached even at the time scale of the experiments. Results from this study demonstrate that infiltration of REE-enriched melt within a mantle peridotite is capable of completely resetting the pristine trace element budget of mantle clinopyroxene.

Received 12 December 2022 | Accepted 20 June 2023 | Published 25 July 2023

Introduction

Porous flow is the main mechanism of melt transport in the deep hot mantle and within the thermal boundary layer. Reaction between mantle minerals and transient melts may strongly affect the mineralogy and chemistry of the upper mantle (*e.g.*, Rampone *et al.*, 2020, and references therein). Modal and chemical changes in mantle peridotite can occur as a result of diffuse porous flow, or by focused melt infiltration related to melt-bearing conduits (dunite channels), or pyroxenitic veins and layers (mantle re-fertilization; *e.g.*, Warren, 2016). Melt-rock reactions are therefore able to modify large portions of the mantle and create chemical and isotopic heterogeneity at different length scales and geological settings.

Changes in mineral abundances and chemistry are mainly controlled by physical parameters, as well as the composition and amount (*i.e.* the melt-rock ratio) of the reacting melt. The interaction between an infiltrating melt and partially molten peridotite is controlled by grain-scale processes that involve dissolution, precipitation, reprecipitation and diffusive exchange between the interstitial melt and surrounding crystals (Liang, 2003). Several numerical and theoretical studies investigated the role and kinetics of these grain-scale processes (*e.g.*, Navon and Stolper, 1987; Hauri, 1997; Van Orman *et al.*, 2002) and laboratory experiments successfully reproduced textural and chemical variations observed in natural mantle samples (*e.g.*, Morgan and Liang, 2005; Van den Bleeken *et al.*, 2010; Wang *et al.*, 2020). However, very few experimental studies have directly investigated the trace element (re-)distribution in mantle minerals resulting from melt-peridotite reaction (Lo Cascio *et al.*, 2008; Yao *et al.*, 2012; Ma and Shaw, 2021) which is mostly due to analytical difficulties in measuring trace element concentrations of fine-grained experimental phases. In particular, the efficiency of melt-rock reaction in modifying or resetting the trace element composition of mantle clinopyroxene, which is the main trace element carrier in spinel peridotites (about 1–2 GPa), still remains to be experimentally evaluated.

We performed high pressure reaction experiments at 1–2 GPa, 1200–1350 °C, on homogeneous mixtures of clinopyroxene (250–160 µm), olivine and an enriched MORB melt (Table S-1 and Fig. S-1; full description of experimental details in Supplementary Information). Initial weight proportions among basalt, clinopyroxene and olivine are 1:1:1, except for one run performed with a mix of 2:1:1, respectively (Table S-2). Such a high melt/rock ratio is consistent with previous melt transport experiments (*e.g.*, Lambart *et al.*, 2009) or melt-peridotite interaction occurring in the host mantle of pyroxenite veins (Bodinier *et al.*, 2004). Adopting a simplified mantle assemblage (olivine + clinopyroxene) promoted the development of coarse textures suitable for the analysis of the trace element composition with laser

1. Dip. Scienze Terra, University of Milano, 20133 Milano, Italy
2. DISTAV, University of Genova, 16132 Genova, Italy
3. Institut fuer Mineralogie, Westfalische Wilhelms Universitat Muenster, Muenster, Germany
* Corresponding author (email: giulio.borghini@unimi.it)

ablation ICP-MS techniques. Here we experimentally determine textural and chemical effects of reactive infiltration/migration of REE-enriched melt within a mantle peridotite with particular focus on REE re-distribution *via* melt-clinopyroxene interaction at asthenosphere-lithosphere conditions.

Melt-Peridotite Reaction Experiments

All experiments produced chemical and textural evidence of the reaction $melt_1 + cpx_1 + ol_1 = melt_2 + cpx_2 + ol_2$, implying the dissolution and recrystallisation of olivine and clinopyroxene (Table S-2). Accordingly, at 1–2 GPa clinopyroxene is the liquidus phase for the selected basaltic glass (Fig. S-2). In the long duration runs (≥48 h), olivine has rather homogeneous major element compositions marked by higher CaO and lower NiO and X_{Mg} [$X_{Mg} = Mg/(Mg + Fe^{tot})$] than the initial SC olivine (Fig. S-3), as observed in basalt-dunite reaction experiments (Borghini *et al.*, 2018). New crystallised clinopyroxene has partially replaced the starting clinopyroxene forming rims on initial clinopyroxene relics or homogeneous grains precipitated by the reacted melt (Fig. 1a, c). New clinopyroxenes have lower Ca and Cr contents and higher Na concentrations with respect to the initial clinopyroxene (Fig. S-2, Tables S-3 and S-4). By contrast, most clinopyroxene relics preserve the initial major element composition (Fig. 1, Tables S-3 and S-4). Al_{IV} content in clinopyroxene varies within a rather narrow range in a single experiment and tends to be higher in the runs with a high degree of crystallisation or a higher initial melt proportion (Fig. S-3). Reacted glasses still retain basaltic major element compositions but exhibit higher X_{Mg} than the initial basalt (Table S-6) due to reaction with mantle phases.

Image analysis, derived by combining X-ray concentration maps, provided estimates of modal variations caused by the reaction (Figs. 1b, S-2 and Table S-2). The degree of clinopyroxene textural replacement (new cpx/relict cpx ratio) increases with temperature and run duration (Fig. 1d). At 1.5 GPa, 1300 °C, and 2 GPa, 1350 °C, clinopyroxene is almost completely renewed by reaction with the melt, in runs of 69 and 48 hours, respectively. The extent of reacted melt crystallisation in experiments increases with increasing pressure and/or decreasing temperature, as demonstrated by the low final melt/rock ratio in experiment at 2 GPa and 1300 °C (Table S1 and Fig. S-2).

REE Distribution after Melt-Cpx Interaction

Consistent with the fast diffusion in silicate melt, experimental glasses have homogeneous trace element concentrations, and show LREE-HREE fractionation ($La_N/Yb_N = 1.74–3.66$) slightly lower than the initial glass ($La_N/Yb_N = 5.49$), mostly reflecting the dissolution of LREE-depleted clinopyroxene (Table S-9). Compared to the starting clinopyroxene, the new clinopyroxenes

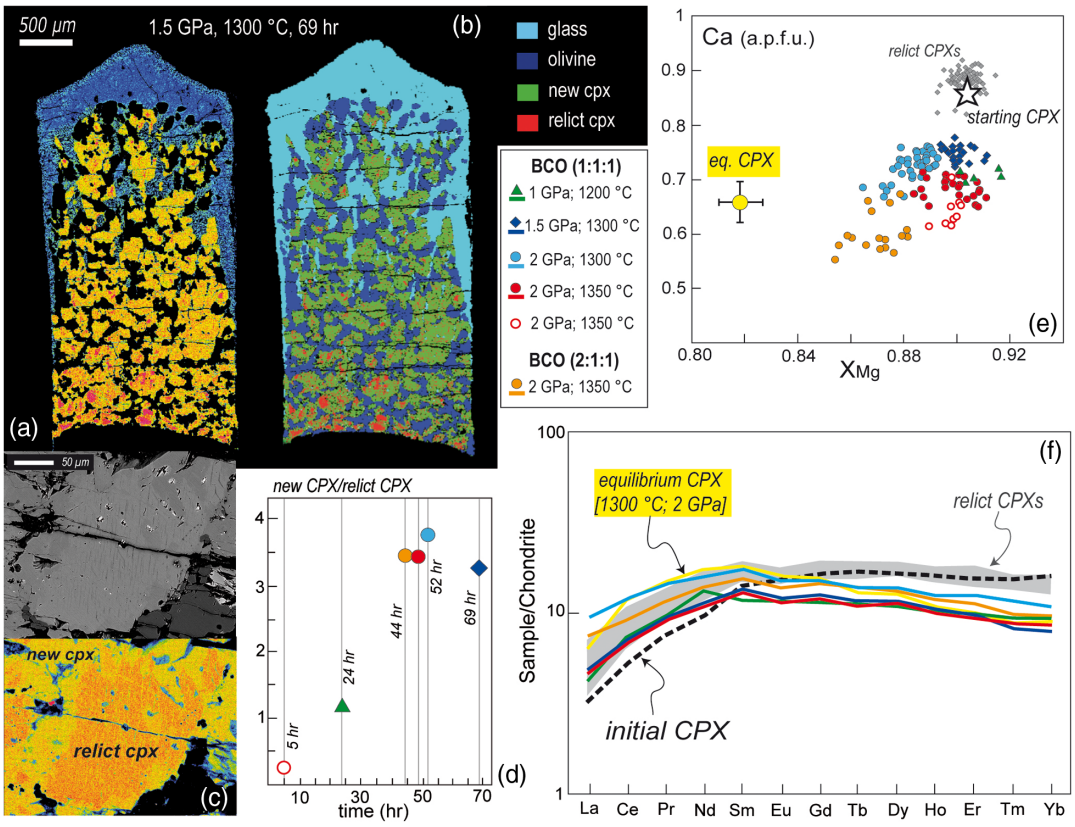

Figure 1 **(a)** Map of Ca distribution in the whole capsule after reaction experiments on Basalt:Clinopyroxene:Olivine (BCO) 1:1:1, at 1.5 GPa and 1300 °C; red areas (high Ca) depict relicts of starting clinopyroxene. **(b)** Phase map derived by combining X-ray concentration maps (Ca, Mg, Al). **(c)** Backscattered electron (BSE) image and Ca map showing details of Ca-rich relict clinopyroxene that is partially substituted by rims of new crystallised clinopyroxene. **(d)** New cpx/relict cpx ratio (*i.e.* clinopyroxene textural replacement) *versus* run duration of experiments (time, hours). **(e)** Ca (a.p.f.u.) *versus* X_{Mg} value [$Mg/(Mg + Fe_{tot})$] of starting, new and relict clinopyroxenes in reaction experiments; also shown is the composition of clynopyroxene in equilibrium crystallisation experiments at 2 GPa and 1300 °C. **(f)** Chondrite normalized REE patterns of average clinopyroxene in reaction and crystallisation experiments compared to the average REE pattern of starting clinopyroxene; grey field is defined by REE patterns of relict clinopyroxenes.

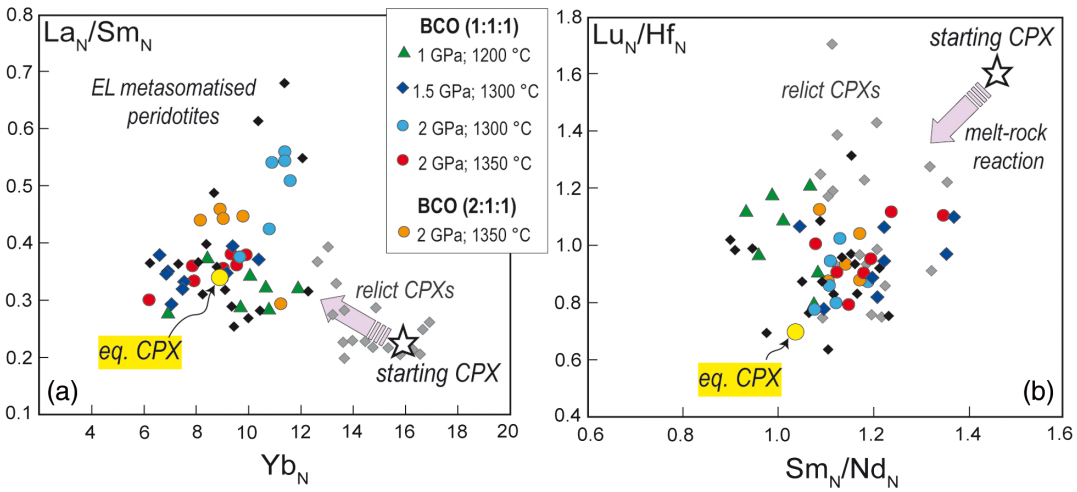

Figure 2 Chondrite normalised **(a)** La_N/Sm_N *versus* Yb_N and **(b)** Sm_N/Nd_N *versus* Lu_N/Hf_N of initial, new and relict clinopyroxene from reacted and crystallisation experiments compared to data of clinopyroxenes in metasomatised peridotites from Northern Apennine veined mantle (black diamonds, Borghini *et al.*, 2020).

show REE patterns characterised by a systematic lowering of HREE and MREE and increasing fractionation of LREE over the MREE reflecting the crystallisation from enriched reacted melts (Fig. 1f). Remarkably, relict clinopyroxenes are modified; the slight but systematic LREE (and Sm) enrichment compared to the starting clinopyroxene (Fig. 1f) reflects partial REE re-equilibration *via* diffusion presumably driven by the more pronounced difference in LREE concentration between initial clinopyroxene and melt, at rather close HREE abundances. REE diffusion within cpx relics coincides with dissolution and precipitation during the interaction with melts (Lo Cascio *et al.*, 2008). Theoretical studies revealed that REE fractionation *via* diffusion is rather sluggish during melt porous flow (*e.g.*, Van Orman *et al.*, 2002; Liang, 2003). However, REE diffusion over a distance of less than 200 μm has been observed in reaction couple experiments (Lo Cascio *et al.*, 2008). In our experimental setup both dissolution and reprecipitation and solid-liquid REE diffusion into the relict clinopyroxenes occur, thus resulting in the whole chemical modification of the initial mantle clinopyroxene at sizes lower than 250 μm, along 2–3 day experiments. These results indicate that rapid textural replacement of relict clinopyroxene strongly improves trace element remobilisation, even for LREE having low diffusion rate (Van Orman *et al.*, 2001).

New clinopyroxenes show clockwise-rotated average REE patterns (Fig. 1f), very similar to REE patterns computed in studies that documented the effect of interaction between enriched melts and residual clinopyroxene within pyroxenite-bearing veined peridotite (Borghini *et al.*, 2020), or during melt infiltration during open system mantle melting, to explain the trace element variability of abyssal peridotite (Brunelli *et al.*, 2014). We found that the fractionation of LREE over the MREE varies as a function of experimental conditions. In particular, clinopyroxenes in experiments that experienced the highest extent of reacted melt crystallisation at 2 GPa and 1300 °C (Fig. 2a) exhibit high La_N/Sm_N ratios ($La_N/Sm_N = 0.42–0.56$), reflecting REE fractionation of crystallising reacted melt. Moreover, high La_N/Sm_N ratios in new clinopyroxenes have been found in the reaction experiment with a higher amount of starting basalt. Similar high La_N/Sm_N ratios have been documented in mantle peridotites inferred to be metasomatised by E-MORB-like melts coming from pyroxenitic veins (Northern Apennine veined mantle; Borghini *et al.*, 2020). Ancient events of melt infiltration in those peridotites modified the trace element composition of clinopyroxene by lowering Sm_N/Nd_N and Lu_N/Hf_N ratios that, over time, formed mantle domains with enriched Nd-Hf isotopic signatures (Borghini *et al.*, 2021). Our experimental results show that high pressure and temperature interaction with E-MORB-type basalt causes rapid decrease of Sm_N/Nd_N and Lu_N/Hf_N ratios in newly formed clinopyroxene relative to the starting

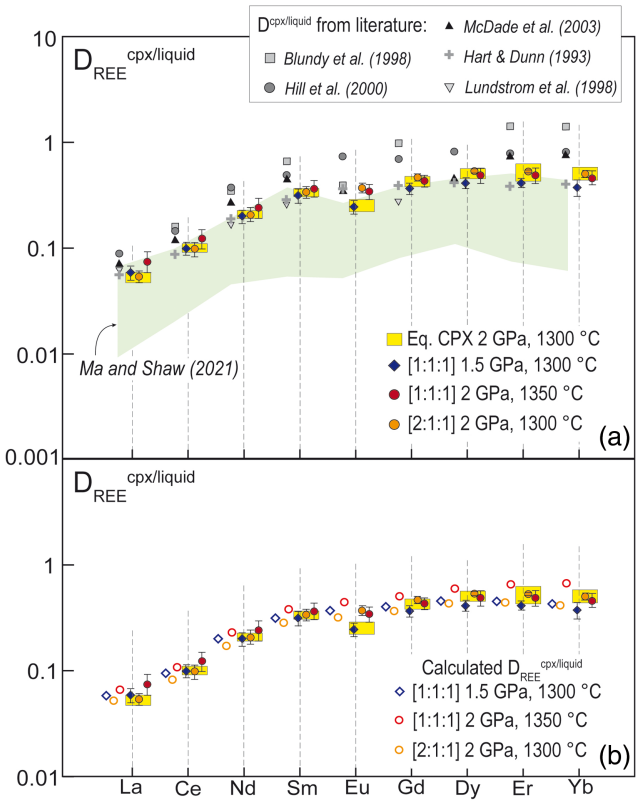

Figure 3 "Reaction" $D_{REE}^{cpx/liquid}$ from this study compared to **(a)** $D_{REE}^{cpx/liquid}$ derived by equilibrium crystallisation experiment at 2 GPa and 1300 °C and those from the literature (list of references is in the text), and **(b)** the $D_{REE}^{cpx/liquid}$ provided by the application of the parameterised lattice strain model by Sun and Liang (2012), to each reaction experiments of this study.

composition (Fig. 2b). In addition, diffusion combined with dissolution and reprecipitation results in variable but systematic chemical changes in clinopyroxene relics, again towards lower Sm_N/Nd_N and Lu_N/Hf_N ratios (Fig. 2b).

Using the REE concentrations measured in new clinopyroxenes and texturally associated glasses, we computed "reaction" cpx/melt distribution coefficients (Fig. 3a), which are comparable to those derived by equilibrium experiments (Hart and Dunn, 1993; Blundy *et al.*, 1998; Lundstrom *et al.*, 1998; Hill *et al.*, 2000; McDade *et al.*, 2003). These also closely overlap the equilibrium distribution coefficients measured for REE in our crystallisation run at 2 GPa and 1300 °C and those computed using parameterisation by Sun and Liang (2012) based on the composition of clinopyroxenes in our reaction experiments (Fig. 3b). This suggests that new clinopyroxenes and reacted melt approached the chemical equilibrium even at the time scale of the experiment. These experiments reveal that small (<250 μm) mantle clinopyroxene is rapidly modified by a single step of interaction with a REE-enriched transient melt. In a scenario of multiple melt injections, porous migration of melts enriched in trace elements may efficiently refertilise mantle clinopyroxene (*e.g.*, Brunelli *et al.*, 2014). Several interactions with REE-depleted clinopyroxene are expected to progressively smooth the LREE-HREE fractionation of a single batch of transient melt, as found in reacted glasses of this study, confirming the important role of melt transport processes in the chemical variations of erupted basalts (Navon and Stolper, 1987).

Conclusions

New experimental results demonstrate that melt-peridotite reaction is efficient in modifying the REE signature of mantle clinopyroxene by a combination of dissolution, precipitation and trace element diffusion. High reaction rate leads to local chemical equilibrium between clinopyroxene and melt even at the time scale of the experiments. These data demonstrate that infiltration of REE-enriched melt within a mantle peridotite is potentially able to completely reset the pristine trace element budget of clinopyroxene.

Acknowledgements

We thank two anonymous reviewers for constructive reviews and Anat Shahar for editorial handling. We greatly thank A. Cipriani for providing the starting basaltic glass. A. Risplendente and G. Sessa are thanked for technical assistance during the work at the electron microprobe and LA-ICP-MS, respectively, at University of Milano. Our thanks also go to B. Schmitte at the University of Münster for her excellent support during the LA-ICP-MS analyses that were done in the midst of the international Covid19 pandemic.

Editor: Anat Shahar

Additional Information

Supplementary Information accompanies this letter at https://www.geochemicalperspectivesletters.org/article2323.

Cite this letter as: Borghini, G., Fumagalli, P., Arrigoni, F., Rampone, E., Berndt, J., Klemme, S., Tiepolo, M. (2023) Fast REE re-distribution in mantle clinopyroxene *via* reactive melt infiltration. *Geochem. Persp. Let.* 26, 40–44. https://doi.org/10.7185/geochemlet.2323

References

Blundy, J.D., Robinson, J.A.C., Wood, B.J. (1998) Heavy REE are compatible in clinopyroxene on the spinel lherzolite solidus. *Earth and Planetary Science Letters* 160, 493–504. https://doi.org/10.1016/S0012-821X(98)00106-X

Bodinier, J.-L., Menzies, M.A., Shimizu, N., Frey, F.A., McPherson, E. (2004) Silicate, Hydrous and Carbonate Metasomatism at Lherz, France: Contemporaneous Derivatives of Silicate Melt–Harzburgite Reaction. *Journal of Petrology* 45, 299–320. https://doi.org/10.1093/petrology/egg107

Borghini, G., Francomme, J.E., Fumagalli, P. (2018) Melt-dunite interactions at 0.5 and 0.7 GPa: experimental constraints on the origin of olivine-rich troctolites. *Lithos* 323, 44–57. https://doi.org/10.1016/j.lithos.2018.09.022

Borghini, G., Rampone, E., Zanetti, A., Class, C., Fumagalli, P., Godard, M. (2020) Ligurian pyroxenite-peridotite sequences (Italy) and the role of melt-rock reaction in creating enriched-MORB mantle sources. *Chemical Geology* 532, 119252. https://doi.org/10.1016/j.chemgeo.2019.07.027

Borghini, G., Rampone, E., Class, C., Goldstein, S., Cai, Y., Cipriani, A., Hofmann, A.W., Bolge, L. (2021) Enriched Hf–Nd isotopic signature of veined pyroxenite-infiltrated peridotite as a possible source for E-MORB. *Chemical Geology* 586, 120591. https://doi.org/10.1016/j.chemgeo.2021.120591

Brunelli, D., Paganelli, E., Seyler, M. (2014) Percolation of enriched melts during incremental open-system melting in the spinel field: A REE approach to abyssal peridotites from the Southwest Indian Ridge. *Geochimica et Cosmochimica Acta* 127, 190–203. https://doi.org/10.1016/j.gca.2013.11.040

Hart, S.R., Dunn, T. (1993) Experimental cpx/melt partitioning of 24 trace elements. *Contributions to Mineralogy and Petrology* 113, 1–8. https://doi.org/10.1007/BF00320827

Hauri, E.H. (1997) Melt migration and mantle chromatography, 1: simplified theory and conditions for chemical and isotopic decoupling. *Earth and Planetary Science Letters* 153, 1–19. https://doi.org/10.1016/S0012-821X(97)00157-X

Hill, E., Wood, B.J., Blundy, J.D. (2000) The effect of Ca-Tschermaks component on trace element partitioning between clinopyroxene and silicate melt. *Lithos* 53, 203–215. https://doi.org/10.1016/S0024-4937(00)00025-6

Lambart, S., Laporte, D., Schiano, P. (2009) An experimental study of focused magma transport and basalt–peridotite interactions beneath mid-ocean ridges: implications for the generation of primitive MORB compositions. *Contributions to Mineralogy and Petrology* 157, 429–451. https://doi.org/10.1007/s00410-008-0344-7

Liang, Y. (2003) Kinetics of crystal-melt reaction in partially molten silicates: 1. Grain scale processes. *Geochemistry, Geophysics, Geosystems* 4, 1045. https://doi.org/10.1029/2002GC000375

Lo Cascio, M., Liang, Y., Shimizu, N., Hess, P.C. (2008) An experimental study of the grain-scale processes of peridotite melting: implications for major and trace element distribution during equilibrium and disequilibrium melting. *Contributions to Mineralogy and Petrology* 156, 87–102. https://doi.org/10.1007/s00410-007-0275-8

Lundstrom, C.C., Shaw, H.F., Ryerson, F.J., Williams, Q., Gill, J. (1998) Crystal chemical control of clinopyroxene-melt partitioning in the Di-Ab-An system: implications for elemental fractionations in the depleted mantle. *Geochimimica et Cosmochimica Acta* 62, 2849–2862. https://doi.org/10.1016/S0016-7037(98)00197-5

Ma, S., Shaw, C.S.J. (2021) An Experimental Study of Trace Element Partitioning between Peridotite Minerals and Alkaline Basaltic Melts at 1250°C and 1 GPa: Crystal and Melt Composition Impacts on Partition Coefficients. *Journal of Petrology* 62, egab084. https://doi.org/10.1093/petrology/egab084

McDade, P., Blundy, J.D., Wood, B.J. (2003) Trace element partitioning on the Tinaquillo Lherzolite solidus at 1.5 GPa. *Physics of the Earth and Planetary Interiors* 139, 129–147. https://doi.org/10.1016/S0031-9201(03)00149-3

Morgan, Z., Liang, Y. (2005) An experimental study of the kinetics of lherzolite reactive dissolution with applications to melt channel formation. *Contributions to Mineralogy and Petrology* 150, 369–385. https://doi.org/10.1007/s00410-005-0033-8

Navon, O., Stolper, E. (1987) Geochemical Consequences of Melt Percolation: The Upper Mantle as a Chromatographic Column. *The Journal of Geology* 95, 285–307. https://doi.org/10.1086/629131

Rampone, E., Borghini, G., Basch, V. (2020) Melt migration and melt-rock reaction in the Alpine-Apennine peridotites: Insights on mantle dynamics in extending lithosphere. *Geoscience Frontiers* 11, 151–166. https://doi.org/10.1016/j.gsf.2018.11.001

Sun, C., Liang, Y. (2012) Distribution of REE between clinopyroxene and basaltic melt along a mantle adiabat: effects of major element composition, water, and temperature. *Contributions to Mineralogy and Petrology* 163, 807–823. https://doi.org/10.1007/s00410-011-0700-x

Van Den Bleeken, G., Müntener, O., Ulmer, P. (2010) Reaction Processes between Tholeiitic Melt and Residual Peridotite in the Uppermost Mantle: an Experimental Study at 0.8 GPa. *Journal of Petrology* 51, 153–183. https://doi.org/10.1093/petrology/egp066

Van Orman, J.A., Grove, T.L., Shimizu, N. (2001) Rare earth element diffusion in diopside: influence of temperature, pressure, and ionic radius, and an elastic model for diffusion in silicates. *Contributions to Mineralogy and Petrology* 141, 687–703. https://doi.org/10.1007/s004100100269

Van Orman, J.A., Grove, T.L., Shimizu, N. (2002) Diffusive fractionation of trace elements during production and transport of melt in Earth's upper mantle. *Earth and Planetary Science Letters* 198, 93–112. https://doi.org/10.1016/S0012-821X(02)00492-2

Wang, C., Lo Cascio, M., Liang, Y., Xu, W. (2020) An experimental study of peridotite dissolution in eclogite-derived melts: Implications for styles of melt-rock interaction in lithospheric mantle beneath the North China Craton. *Geochimica et Cosmochimica Acta* 278, 157–176. https://doi.org/10.1016/j.gca.2019.09.022

Warren, J.M. (2016) Global variations in abyssal peridotite compositions. *Lithos* 248–251, 193–219. http://dx.doi.org/10.1016/j.lithos.2015.12.023

Yao, L., Sun, C., Liang, Y. (2012) A parameterized model for REE distribution between low-Ca pyroxene and basaltic melts with applications to REE partitioning in low-Ca pyroxene along a mantle adiabat and during pyroxenite-derived melt and peridotite interaction. *Contributions to Mineralogy and Petrology* 164, 261–280. https://doi.org/10.1007/s00410-012-0737-5